Mechanical Properties

Large Strain Behavior

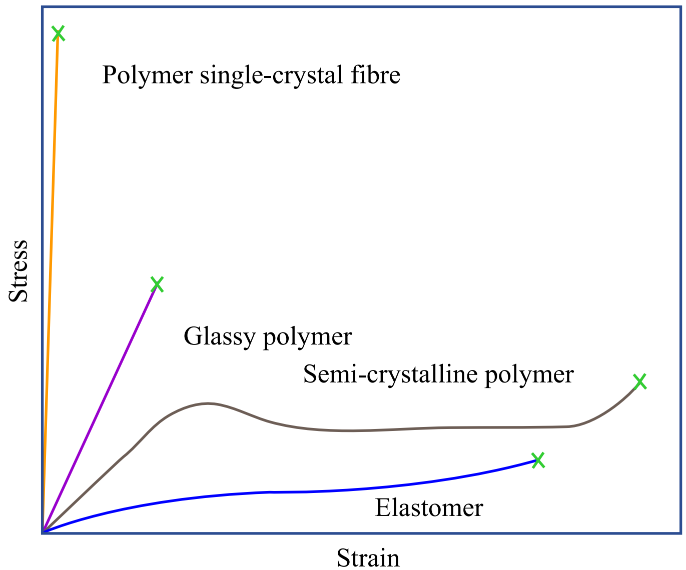

Schematic stress-strain curves of different types of polymers, drawn approximately to scale.

Figure by MIT OCW.

Polymeric Behavior

- Gels
- Elastomers
- Glasses
- Semicrystalline
- Fibers

Types of Polymer	Young's Modulus (N/m^2)
Gel	$\sim 10^3$
Elastomer	$\sim 10^6$
Glassy polymer	$\sim 10^9$
Polymer crystal ($\perp$, // to c)	$\sim 10^9, 10^{11}$
SWCNT (‖ to c)	$\sim 10^{12}$

- Large anisotropy of bonding: covalent vs. secondary
- Homogeneous vs. heterogeneous microstructures
- Microstructure: amount, size, shape, orientation and connectivity-topology
- Large (huge) changes in microstructure with deformation

Localized Deformation in Polymers

- **1. Crazing (dilational deformation)**
- **2. Shear banding (constant volume deformation)**

<u>Crazes</u> (for glassy polymers, micronecks for semiXLine polymers)

Orient perpendicular to principal tensile stress

<u>Shear Bands</u>

Orient along directions of principal shear stress

Shear Yielding

$\Delta V \cong 0$

$\varepsilon_y^{\text{metals}} \sim 0.1\%$

$\varepsilon_y^{\text{polymer}} \sim 5\text{-}10\%$

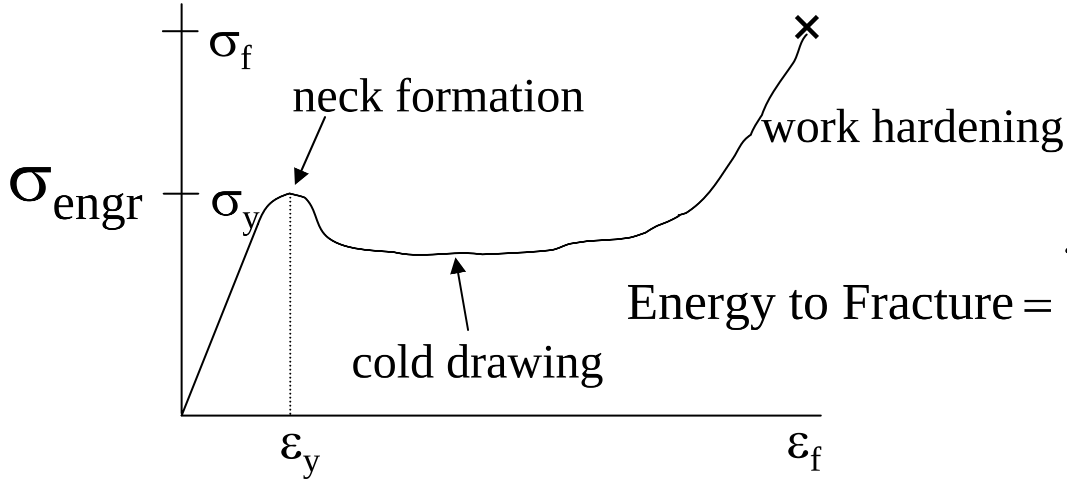

$$\text{Energy to Fracture} = \int_0^{\varepsilon_f} \sigma \, d\varepsilon$$

Necking: reduction in sample x-sectional area

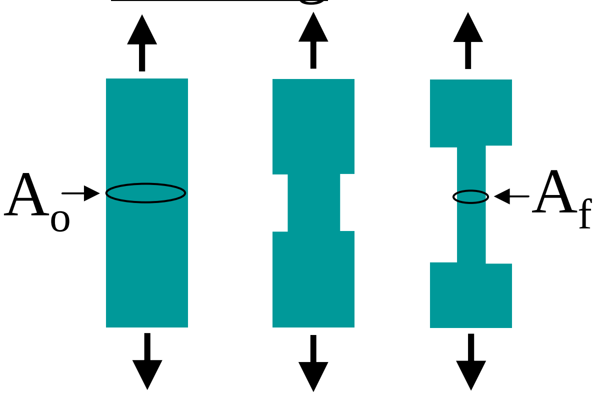

$$\lambda_{draw} = \frac{A_o}{A_f} = \frac{l_f}{l_o}$$

True stress ≥ Engr stress. Therefore necked region must be stronger (by a factor of λ) than un-necked region of sample.

Strain Hardening in Polymers

$\frac{d\sigma}{d\varepsilon}$ entropic subchains, crystal orientation and crystallization

Polymers - Hydrostatic Pressure Effects

• Tresca and Von Mises treat tension ≅ compression but unlike metals, yield in polymers is quite <u>sensitive to hydrostatic pressure</u>: $P = (1/3)(\sigma_{11} + \sigma_{22} + \sigma_{33})$

Image removed due to copyright restrictions.

Please see Fig. 5.27 in Lovell, Peter A., and Young, Robert Joseph. *Introduction to Polymers.* New York, NY: Chapman and Hall, 1991.

pressure

hydrostatic pressure

$$\sigma_y(P) = \sigma^o_y - \mu P$$

material constant

(-) compression

(+) tension

Viscoelastic/Relaxation:
Interplay of Temperature and Strain Rate

Image removed due to copyright restrictions.

Please see Fig. 5.29 in Lovell, Peter A., and Young, Robert Joseph. *Introduction to Polymers.* New York, NY: Chapman and Hall, 1991.

PMMA

$\sigma_y \uparrow$ with $\uparrow \dot{\varepsilon}$

$\sigma_y \uparrow$ with $\downarrow T$

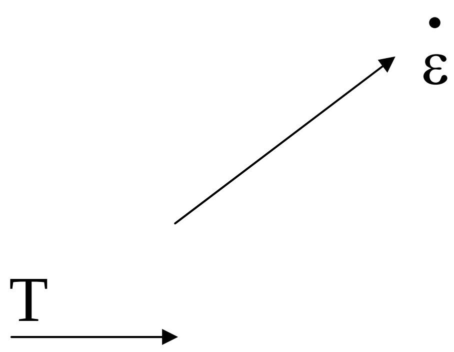

- Response of sub-chains to rate of loading

Craze Yielding

$\Delta V > 0$ dilation/cavitation – void formation under tension

- nucleation @ flaws – usually at surface
- crazing only occurs for (+) hydrostatic tensile stress state
- craze plane forms ⊥ to max principal tensile stress

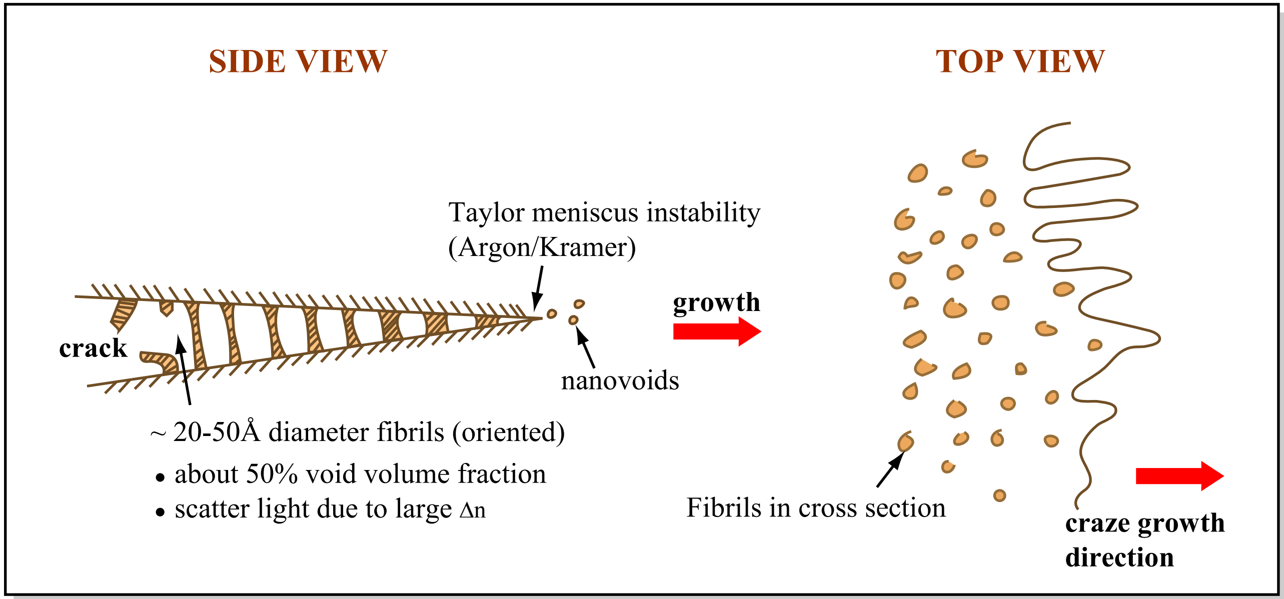

Figure by MIT OCW.

Environmental Crazing Agents

- lower $\gamma_{surface}$
- plasticize

Craze Microstructure

- **Elongated fibril/void network.**
- **Typical void content approximately 50%.**
- **Fibril diameter ~ 5nm, fibril spacing ~ 20nm.**
- **Draw ratio of fibrils is 1/(void volume fraction) ~ 2**
- **Voids form at advancing craze tip due to dilational stresses**
- **Craze tip growth is by Taylor meniscus instability (see schematic) of fingering and fibril pinch-off.**
- **Voids grow and fibrils elongate as polymer chains orient, become drawn into the craze and work harden.**
- **Craze thickens by drawing in new material as well as by further elongation of the fibril (decrease in diameter)**
- **Heating above T_g leads to healing and recovery (entanglement network of subchains).**

Craze Microstructure cont'd

- **Crazes with high void content and a large fibril draw ratio are prone to easy breakdown (crack propagation and brittle fracture).**
- **The draw ratio (λ) of a fibril depends on the contour length (l_e) between entanglements and the distance between entanglements (d_e).**

$$\lambda \approx \frac{le}{\sqrt{de}} \approx \frac{Me/Mo}{\sqrt{Me}} \approx \sqrt{Me}$$

Shear Banding vs. Crazing

- Shear banding occurs if the number of entanglements per chain is large so that the crazing stress is higher than the yield stress.
- Crazing occurs if the yield stress is lower, for example if the molecular weight is low (few entanglements) or the temperature is high (constraint release).

Cellular Materials

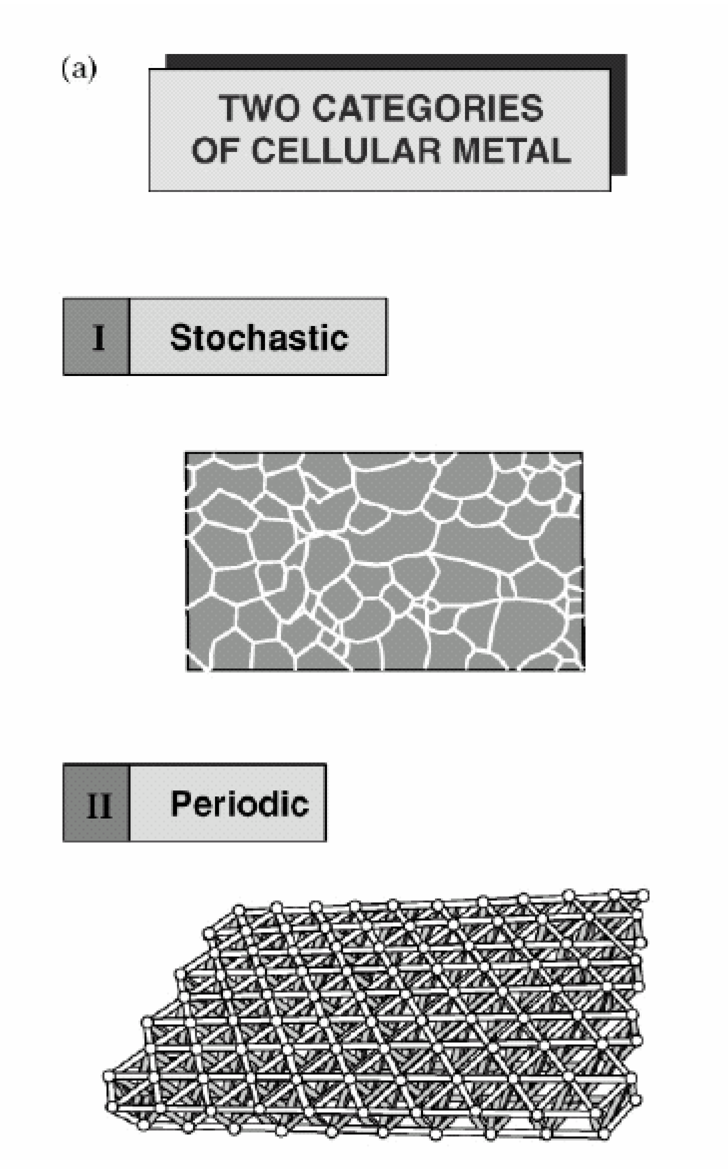

Evans A. G. *et al.*
Progress in Materials Science **46**, 309-32 (2001).

Advantages in ultra-light structures, heat dissipation, vibration control, and energy absorption

Cellular metals have the *highest energy absorption* per unit mass of any material.

Properties of cellular materials are sensitive to the microstructure of the cells.

- **Methods of Fabrication**
- **Establishing relations between Geometry and Performance**
- **Mechanical Behavior of Micro-Nano-Structured Materials**

Random vs Periodic Cellular Materials

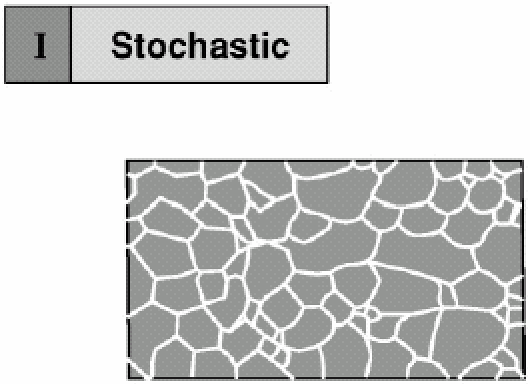

Random Cellular Materials:
Open and closed cell alloy foams.

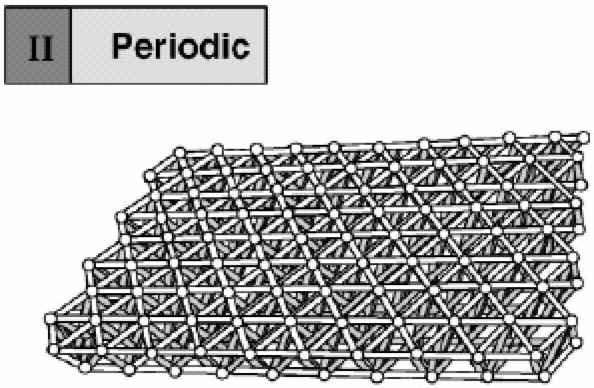

Periodic Cellular Materials:
Structures based on a repeating unit cell.

Periodic cellular solids can be constructed with topologies exhibiting properties greatly superior to those demonstrated by their stochastic analogues at the same volume fraction.

Unlike random materials, periodic cellular solids can be precisely described and their properties accurately calculated.

Periodic Cellular Solids: Modeling, Fabrication and Testing on the same structure.

Evans A. G. *et al.* "The topological design of multifunctional cellular materials"
Progress in Materials Science **46**, 309-32 (2001).

Millitrusses

Lightweight structures comprised of stiff load bearing connections made using as little material as possible.

1. Bending dominated structures
2. Stretch dominated structures - fully triangulated

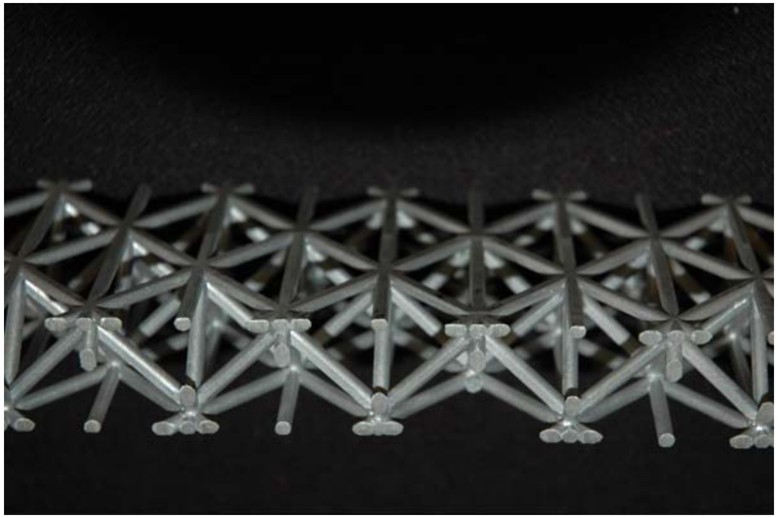

2D

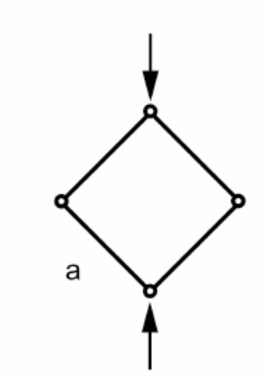

Bending Dominated

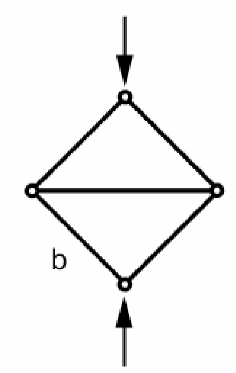

Stretch Dominated

3D

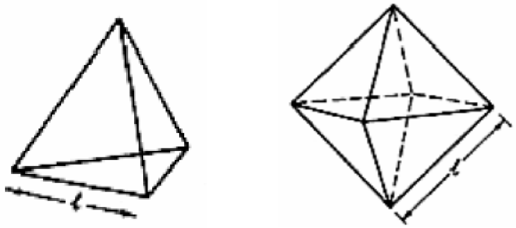

Stretch Dominated

Microframes: **2D & 3D Periodic Materials by Rational Design**

Ultra-light, designer structures by IL

with length scale dependent mechanical behavior

Image removed due to copyright restrictions.

Please see Cover, *Advanced Materials* 18 (August, 2006)

Specified Symmetry and Porosity

Bicontinuous Polymer/Air Structures

Materials:
Negative Tone Resists
Positive Tone Resists

• Stiff, Strong	Variable Xlink Density
• Lightweight	Gradients in Structure, Xlinks
• New Deformation Mechanisms	Ceramic Infill
• Towards Champion Toughness	NP Additives

Multibeam Interference Lithography

- **Idea:** **Interference of light**

  ➔ periodic intensity distribution in a photoresist

- **Length scale:** **500-2000 nm**

- **Accessible architectures:**

  1D, 2D, 3D, quasi crystals

- **Advantages:**

  - Fast and efficient

  - Defect free

  - Control over cell geometry and volume fraction

1. C. K. Ullal *et al.*, J. Opt. Soc. Am. A **20,** 948 (2003).
2. C. K. Ullal et al., Appl. Phys. Lett. Appl. Phys. Lett. 84, 5434 (2004).

Formulation

SU8

- **High aspect-ratio**
- **Mechanical stability**
- **Thermal stability**

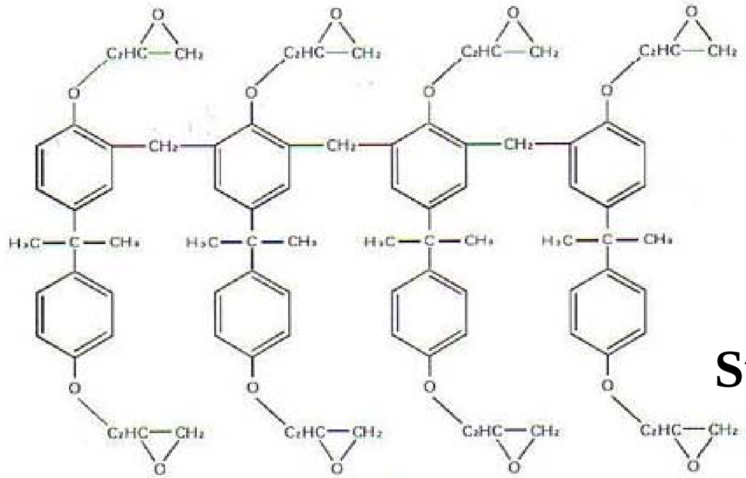

SU-8

+Rubrene (Photoinitiator)
+OPPI (PAGs)
+Base

Supercritical CO_2 drying

Tensile strain of Macroscopic SU8 Samples

Glass Transition Temp. of SU8

- **Uncrosslinked: 50 ^oC**
- **Fully crossliked: 230 ^oC**

Image removed due to copyright restrictions.

Please see Fig. 2 in Feng, Ru, and Farris, Richard J. "Influence of Processing Conditions on the Thermal and Mechanical Properties of SU8 Negative PhotoresistCoatings." *Journal of Micromechanics and Microengineering* 13 (2003): 80-88.

fully crosslinked

Bulk

uncrosslinked

J. Micromech. Microeng. **13** (2003) 80

Choi, T., Jang, J.H., Ullal, C.K., LeMieux, M.C., Tsukruk, V.V., Thomas, E.L., "The Elastic Properties and Plastic Behavior of 2D Polymer Structures Fabricated by Laser Interference Lithography," *Advanced Functional Materials*, 16 (10), 1324-1330 (2006).

2D Microframe: Air Cylinders on Triangular Lattice

2D Interference Lithography

Image removed due to copyright restrictions.

Please see Fig. 1b and c in Gorishnyy, T., et al. “Hypersonic Photonic Crystals.” *Physical Review Letters* 94 (March 25, 2005): 115501.

- Lattice parameter

  a=1360 nm
- Porosity – 39%
- “Single crystal” of SU8

Fabrication of "3 Term Diamond" by 3D Interference Lithography

Images removed due to copyright restrictions.

Please see Fig. 1e in Jang, J.H., et al. "3D Polymer Microframes that Exploit Length-Scale Dependent Mechanical Behavior." *Advanced Materials* 18 (2006): 2123-2127.

Negative Resist (SU8)

J-H. Jang

Templating and Inverting Networks

Polymer/Air

$R\bar{3}m$

Images of bicontinuous networks removed due to copyright restrictions.

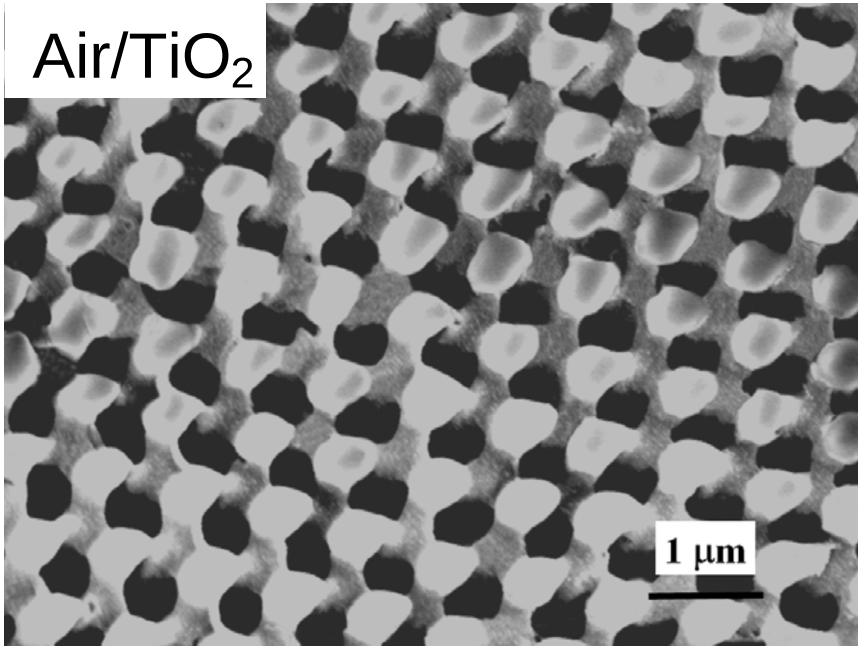

Polymer/Air

$Pm\bar{3}m$

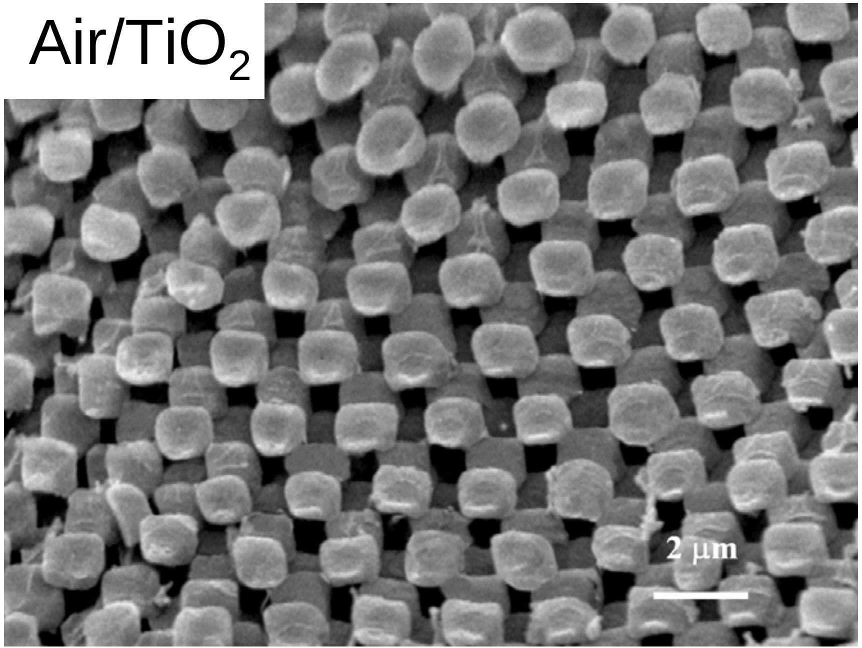

3D Bicontinuous Elastomer/Air Network

3D diamond-like frame fabricated via infil of DMS Monomer into positive resist

Demonstrated length scale reversible/tunable phononics:

3D Elastomeric MechanoPhononic Crystals

Image removed due to copyright restrictions.

Please see Fig. 1 and 2 in Jang, Ji-Hyun, et al. “Mechanically Tunable Three-Dimensional Elastomeric Network/Air Structures via Interference Lithography.” *Nano Letters* 6 (2006): 740-743.

“Millitrusses”

Unit cell

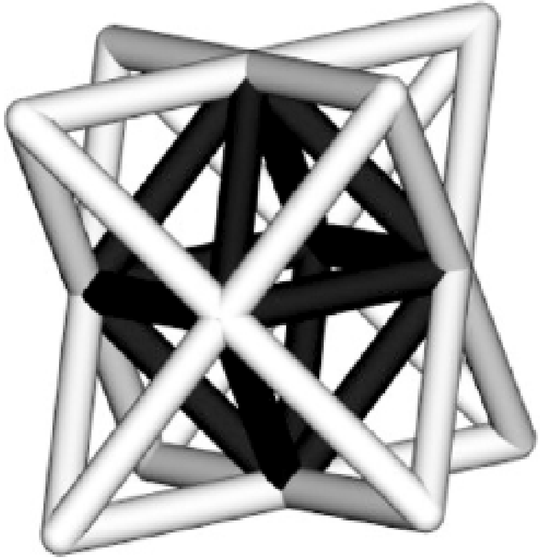

12 connected

Image of extended truss structure
removed due to copyright restrictions.

Inspired by:

J. Hutchinson, M. Ashby, T. Evans, H. Wadley

Designs: 12-Connected Stretch Dominated Structures

Octo-Truss Structure

(Red Curves)

Inverse FR-D IL Structure

(Blue Curves)

Please see: Fig. 3 in Maldovan, Martin, et al. "Sub-Micrometer Scale Periodic Porous Cellular Surfaces: Microframes Produced by Holographic Interference Lithography." *Advanced Materials* 19 (2007): 3809-3813.

Experimental Realization and FEM (linear) of P Microframe

6-connected

Single P

Tubular P

Images removed due to copyright restrictions.
Please see: Fig. 4 in Maldovan, Martin, et al. "Sub-Micrometer Scale Periodic Porous Cellular Surfaces: Microframes Produced by Holographic Interference Lithography." *Advanced Materials* 19 (2007): 3809-3813.

Single P (0.21 to 0.79)

Tubular P (solid line) , Single P (Dots)

3D Microframe with 200 nm feature size - Large Strain Deformation

Images removed due to copyright restrictions.

Please see Fig. 1c, d, and e in Jang, J.H., et al. "3D Polymer Microframes that Exploit Length-Scale Dependent Mechanical Behavior." *Advanced Materials* 18 (2006): 2123-2127.

- **L/D ~ 3.2 for struts**
  ~ 2.3 for posts

- **Density ~ 0.3 gm/cm^3**

Large Strain Deformation Modes of Microframe

Peel Test

Images removed due to copyright restrictions.

Please see Fig. 2b, c, 3b, and c in Jang, J.H., et al. “3D Polymer Microframes that Exploit Length-Scale Dependent Mechanical Behavior.” *Advanced Materials* 18 (2006): 2123-2127.

Mechanical Properties of SU8

1. SU-8: negative photoresist; used in MEMS applications.

Tensile test results of 130 μm SU-8 film:

Image removed due to copyright restriction.

Please see Fig. 2 in Feng, Ru, and Ferris, Richard J. "Influence of Processing Conditions on the Thermal and Mechanical Properties of SU8 Negative Photoresist Coatings." *Journal of Micromechanics and Microengineering* 13 (2003): 80-88.

(200 °C)

(95 °C)

Bulk

6%

NanoFrame

300%

Images removed due to copyright restrictions.

Please see Fig. 3b in Jang, J.H., et al. "3D Polymer Microframes that Exploit Length-Scale Dependent Mechanical Behavior." *Advanced Materials* 18 (2006): 2123-2127.

Fabrication of SU-8 "fibers" using photolithography

1. Spin-coat SU-8 on Si substrates.

 (SU-8 2025: 25 μm, SU-8 2002: 2 μm, and SU-8 200.5: 0.5 μm)

2. Soft bake: 65 °C, 1 min; 95 °C 3 min.

3. Exposure: λ=365 nm; total dose: 270 mJ/cm^2.

 (A mask is an array of windows having a length of 1 mm and variable line widths of 25 μm, 2 μm, and 1 μm.)

4. Post-exposure bake: 65 °C, 1 min; 95 °C, 1 min.

5. Develop.

6. Hard bake: 180 °C 5 min.

Cross-sectional SEM images of the fibers:

Images of SU8 fibers removed due to copyright restrictions.

27 μm

20 μm

24 μm

1.6 μm

1.65 μm

0.5 μm

1 μm

Diameter:	25 μm	1.8 μm	0.7 μm

Get Simple: Tensile Behavior of SU8 "Fibers"

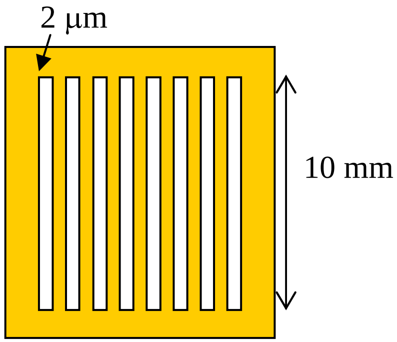

- •Spin coat SU-8 on silicon substrates
- •Soft bake: 65 ^oC, 1 min; 95 ^oC 3 min.
- •Exposure: λ: 365 nm; total dose: 270 mJ/cm^2.
- •Develop: SU-8 developer (from Microchem Corporation).
- •Post-exposure bake: 65 ^oC, 1 min; 95 ^oC, 1 min.
- •Hard bake: 180 ^oC 5 min.

Image of experimental apparatus removed due to copyright restrictions.

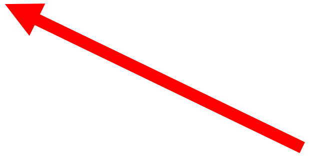

Cardboard template & fi

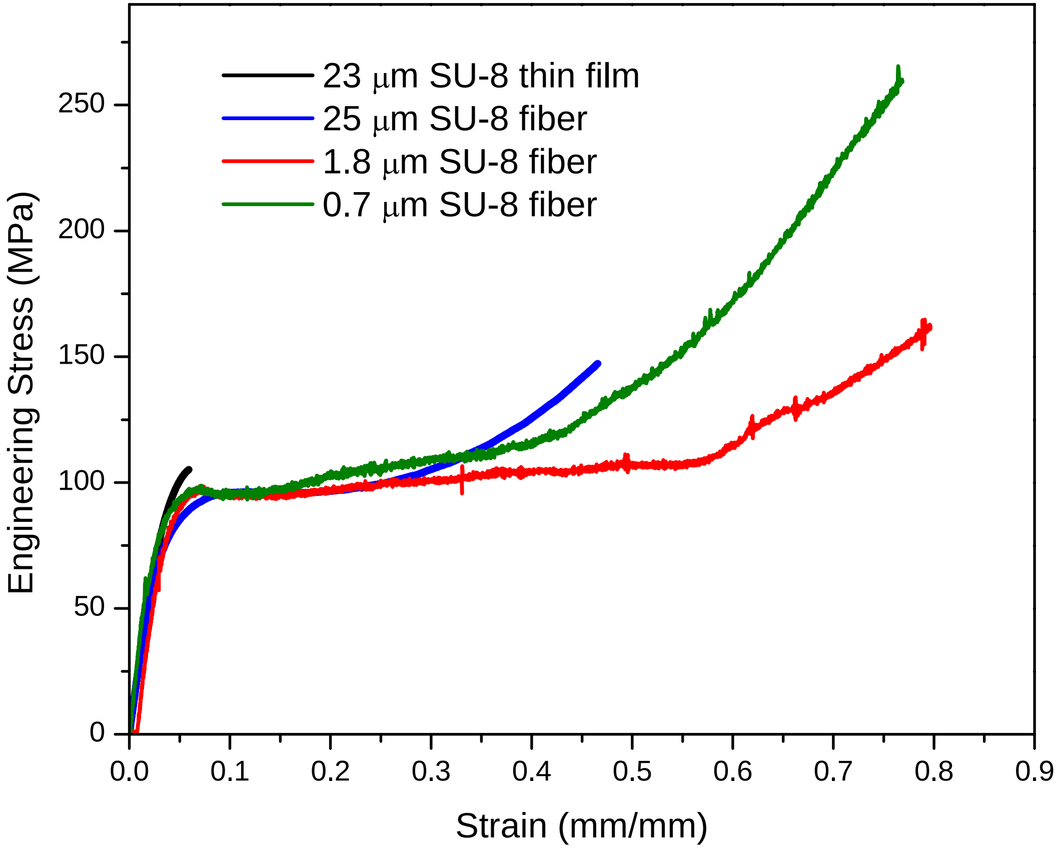

Tensile Test Results of SU-8 fibers

Without hard-baking

With hard-baking (180 ^{o}C, 5 min)

Stress-strain curves removed due to copyright restrictions.

Summary of SU8 Tensile Test Results

Toughness

Material	Kevlar	Polycarbonate	25 μm SU-8 fiber	1.8 μm SU-8 fiber	0.7 μm SU-8 fiber
Toughness (MPa)	120 ± 3.2	60	44 ± 0.5	72.5 ± 2.7	85.4 ± 3.3

Modulus

Plot of Young's modulus against fiber diameter removed due to copyright restrictions.

SU-8 film

Micromechanics of Tensile Deformation

Microscopic response under tension

Actual Sample

Model

Images of simulated deformation and stress-strain curve removed due to copyright restrictions.

Image removed due to copyright restrictions.

Please see Fig. 3b in Jang, J.H., et al. “3D Polymer Microframes that Exploit Length-Scale Dependent Mechanical Behavior.” *Advanced Materials* 18 (2006): 2123-2127.

Lessons Learned

- Red indicates material deforming
- Blue indicates material not deforming
- Small scale of epoxy makes it deformable
- Micro-frame geometry creates multiple deformation domains which spread the deformation through the structure